Multi-axis loading tests on a small-scale tree roots model

G. Marrazzo
Politecnico di Milano, Milan, Italy, giacomo.marrazzo@polimi.it

M.O. Ciantia, T. Riccio, J.A. Knappett
Università degli Studi di Milano-Bicocca, Milan, Italy, matteo.ciantia@unimib.it, University of Dundee, Dundee, Scotland, m.o.ciantia@dundee.ac.uk, 140007677@dundee.ac.uk, J.A.Knappett@dundee.ac.uk

A. Galli
Politecnico di Milano, Milan, Italy, andrea.galli@polimi.it

ABSTRACT: Trees can be considered as "living structures", subjected to a complex combination of vertical, horizontal and toppling loads, mainly deriving from tree self-weight and external actions (e.g. wind). From a geotechnical perspective, the root plate works as a shallow foundation, providing the tree anchoring resistance within the soil. This paper presents a small-scale 1g testing campaign aimed at investigating root plate-soil interaction by means of a new multi-axis loading frame. A 3D printed simplified root model embedded in a medium dense sand is subjected to displacement controlled loading paths, combining vertical and toppling actions. The experimental data are then interpreted in the light of the well-known macroelement theory, and the discussion suggests that such method could be used to reproduce the system mechanical response for different loading directions. The bases of the definition of (i) the limit locus, (ii) the hardening rule and (iii) the plastic potential are also concisely presented.

1. INTRODUCTION

The interest in modelling the mechanical interaction between tree root plates and the surrounding soil is largely increasing in the last decades. New and improved site investigation approaches (e.g. the use of georadar techniques to reconstruct root architecture, Alani and Lantini, 2020; or cork-screw tests for rooted soil characterization, Meijer et al., 2018) and the need to properly face climate change effects on the stability of trees are central issues in this field. Toppling failure mechanisms represent a noticeable source of risk, especially in urban areas where tree collapses may cause severe damage to both people and infrastructures. A multi-disciplinary approach, combining botanic, agronomic and engineering competences would in general be required to address this problem and, in this perspective, Geotechnical Engineers may provide a valuable contribution.

Several experimental works have been proposed since the mid-nineties (Guitard and Castera, 1995; Zhang et al., 2020 and 2023), investigating the moment-rotation curve of trees under specific actions (see also Galli et al., 2023 and Marsiglia et al., 2023), together with numerical modelling works (Dupuy et al., 2005; Yang et al., 2014), but the combined effects of different loading components have only rarely been studied. The preliminary results of a 1g testing campaign on a small-scale simplified 3D root model are here presented. The system was subject to a combined loading condition using a new multi-axis loading frame, under displacement-controlled conditions. From a geotechnical perspective, the root system plays the role of a "living foundation" for the tree, and its behaviour under vertical (both pushing and pulling actions have been considered) and lateral loads are investigated. The experimental results have been evaluated in the light of the well-known macroelement theory (Nova and Montrasio, 1991) originally proposed for shallow foundations in sand.

2. TESTING APPARATUS AND SAMPLE PREPARATION

2.1. The ICE-PICK Apparatus

The tests were performed by means of a new ICE-PICK multi-axis loading frame, which is able to impose maximum vertical and transversal loads of ±5 and 0.5 kN, respectively. DC motors, controlled by a software-based PID feedback-control system, enable actuation along three different orthogonal directions. The ICE-PICK frame has been used in other studies for testing pile prototypes in soft rock and sand under axial, lateral and cyclic loads (Riccio et al., 2024). In this work, the frame is rigidly connected to a cylindrical testing chamber (diameter=300mm, height=280mm) and hosts the motors imposing the

displacements through a clevis joint. This latter acts as the stem of the tree model and it is rigidly attached to the head of the root system. The top of the stem corresponds then to a freely rotating hinge, where loads are applied (Figure 1). The entire apparatus is also designed to fit an X-ray micro-CT scanner apparatus, not utilised in the study here presented.
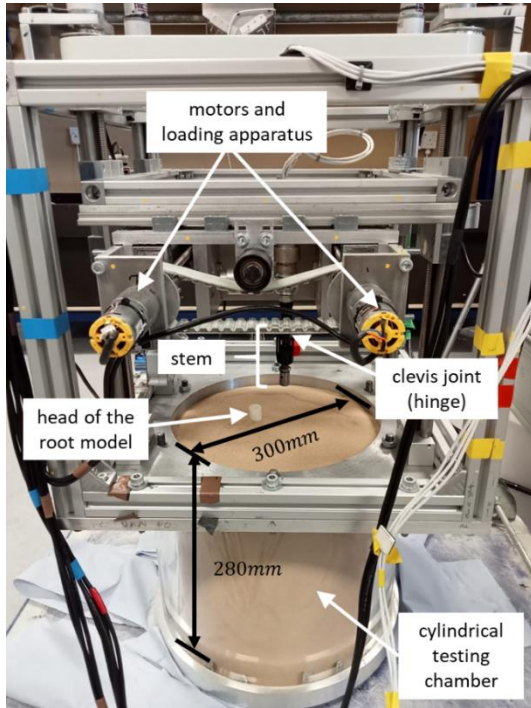

Figure 1. View of the testing apparatus.

2.2. The 3D printed root system

A 1:20 scale 3D printed root model was realised, by using acrylonitrile butadienestyrene plastic (Young's modulus of 650 MPa and Ultimate Tensile Strength of 17 MPa) already employed in mechanical tests on scaled root prototypes (Liang et al., 2014). The geometry is a simplified architecture derived from a complex 3D root of a real tree (Zhang et al., 2023), approximated here by means of equivalent straight elements (Figure 2a). A central tap root (diameter of 6mm and length of 50mm) and lateral and sinker roots (diameters of 3 and 1.6mm, respectively; Figure 2b) have been considered. Thinner parts (e.g. hairy roots) were not here reproduced in order to simplify the manual preparation of the sample, to allow for a better reproducibility of the tests and in view of performing detailed numerical modelling in future studies. Hairy roots are in general characterized by very high tensile strength but, owing to their reduced dimension with respect to other root components, their pull-out resistance is limited and affected by a marked softening behaviour. Their contribution to the overall resisting moment is then in general rather reduced, especially when relatively high values of tilting angles of the tree are reached.

2.3. Model setup

Experimental tests were run using HST95 Congleton silica sand (a uniformly-graded fine sand, employed at University of Dundee in previous works (Liang and Knappett, 2017) and deposited by dry air pluviation at a relative density of 45-50% within the testing chamber, up to a height of 230 mm. The root prototype was then manually positioned and further sand pluviation was conducted to reach a final root embedment d = 15 mm (Figure 2b).
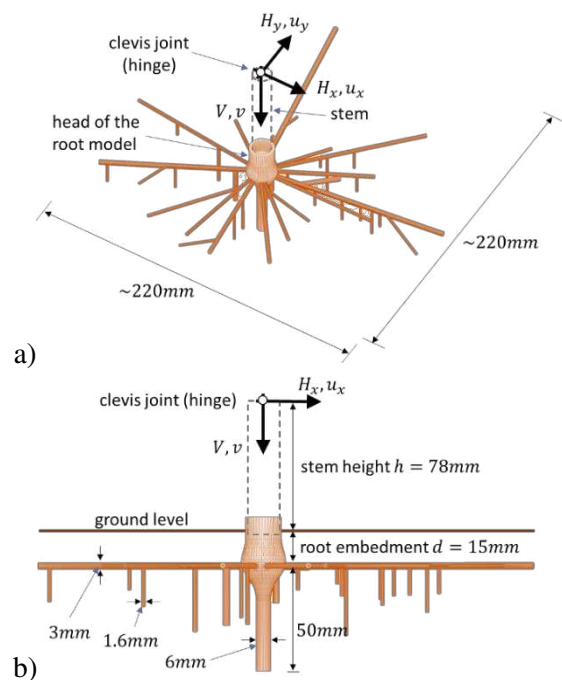

Figure 2. Simplified tree root model: (a) 3D view, and (b) lateral view.

3. LOADING SCHEME

Experimental tests were performed by controlling the vertical (v) and lateral (u_x) displacements of the hinge and by measuring the corresponding reacting force components along the vertical and horizontal directions (V, H_x and H_y, respectively; definitions are indicated in Figure 2a, where negative values of V and v are associated to pull-out tests). The choice of this reference system is consistent with the idea of reproducing the orientation of the on-site dominant wind action on a real tree (Zhang et al., 2023). For the sake of simplicity, the out-of-plane displacement (u_y) was kept equal to zero. Since measurements are in some cases affected by a relatively high noise-to-signal ratio, results will be shown in §4 with reference to a time averaged moving mean over a

time window of 5 seconds (using data sampled at 50 Hz). Four different loading conditions have been considered, ranging from vertical (both compression and pull-out tests, labels 1 and 2, respectively, in Figure 3) to lateral (label 3). An additional complex combined path (label 4) was also considered, consisting in an initial phase with equal increasing trends of v and u_x at the same rate (segment OP; point O does not precisely correspond with the origin of the axes owing to some small inaccuracies in the motor control). A second phase (segment PQ) with a constant continuous increase in u_x at fixed v=10mm was then imposed. This particular path was considered to explore possible coupling effects. The tests were conducted up to relatively high values of final displacement, to incorporate the possible arising of second-order effects. A first set of tests (set a) was run for the four paths at a rate of 0.04 mm/s. Possible rate-dependent effects were also tested by running a second set of tests (set b) at 0.4 mm/s (for paths 1, 2 and 3 only). The two chosen displacement rate values correspond to the minimum and maximum values provided by the motors, respectively. The interpretation of the lateral tests assumed a rigid rotation of the root model at the level of the ground surface. Corresponding toppling moment M_x was then evaluated by multiplying the values of the horizontal force H_x by the lever arm (i.e. the stem height, h=78mm; Figure 2b); the induced rotation ϕ_x was computed as $\tan \phi_x = u_x/h$.
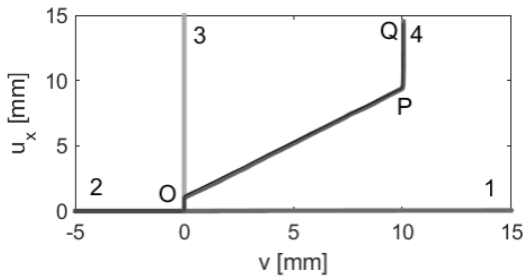

Figure 3. Sketch of the four tested displacement paths.

4. TEST RESULTS

4.1. Lateral tests (path 3)

The results of the lateral tests are shown in Figure 4a. A good quantitative agreement is observed between the curves corresponding with the two imposed displacement rates, with no significant rate-dependent effects. The curves exhibit a marked non-linear behaviour, with a peak resistance of approximately 0.65 Nm at a rotation of about 7.5°. Beyond these points, a ductile behavior with a small decrease in resisting moment was observed.

For the sake of brevity, in Figure 4a a best fitting curve for test a based on equation (1) was here also introduced (see §5 for further comments).
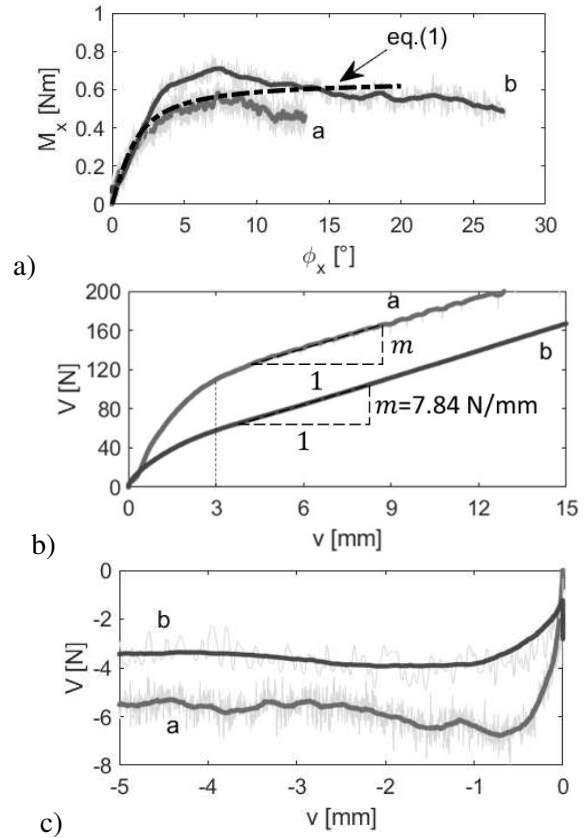

a)

b)

c)

Figure 4. Experimental results: (a) lateral, (b) compression and (c) pull-out tests. Shaded areas represent the rough data and labels a and b refer to the two imposed displacement rates.

4.2. Compression tests (path 1)

The curves of Figure 4b show the results of the vertical compression tests. Evident non-linear trends were obtained, with a marked knee at a vertical settlement of about 3 mm. Beyond this value, an increasing linear trend is observed, associated to the progressive sinking of the roots into the sand, and inducing a continuous increase in the resisting force (similar trends have already been experimentally observed in Marsiglia et al., 2022), characterised by the same gradient m=7.84 N/mm. In this zone, no significant rate-dependent effects are then present. Consistently, the difference in the load values at the knee (~100 N for curve a, and ~60 N for curve b) have also been judged to not depend on the imposed displacement-rate, but only on possible (and unavoidable) inaccuracies during the manual preparation of the sample.

4.3. Pull-out tests (path 2)

Pull-out tests are reported in Figure 4c, where very small values of resisting forces are observed. A pronounced softening behaviour, characterised by a peak value at displacement of –1 mm (negative values stand for uplift displacements) is registered. Owing to the very small values of the loads, inaccuracies due to the manual preparation procedure may play here a more significant role compared to the results of path 1, and any rate-dependent effects cannot be fully clarified.

4.4. Combined test (path 4)

Figure 5 shows the load-displacement curve along the vertical direction and the moment-rotation curve for the test along path 4, respectively. In this case only test set a was considered. In the vertical direction, a non-linear response is observed along the segment OP (although with a less evident knee at ~3 mm with respect to path 1), with larger gradient of 8.4 N/mm (Figure 5a).
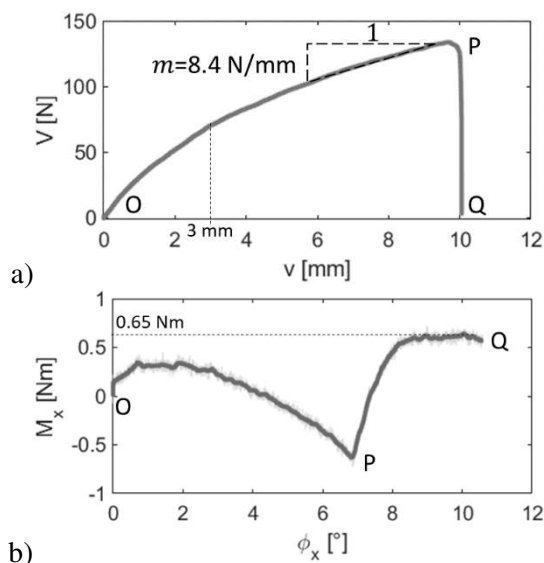

Figure 5. Experimental test results on path 4: (a) vertical load-displacement curve and (b) moment-rotation curve.

This value is approximately consistent with that observed in Figure 4b, and it can be considered representative of the development of significant second order effects. Correspondingly, the values of M_x follow a very complex and non-monotonic response, characterised by an initial increase followed by a complete reduction and even an inversion of the sign (Figure 5b). The subsequent testing phase at fixed v=10mm (segment PQ) shows a complete drop of the vertical load V and, again, a new reverse in the trend of the resisting moment M_x,

with a non-linear increase up to a maximum value of 0.65 Nm.

4.5. Out-of-plane action

For the sake of completeness, the values of the out-of-plane action H_y (not controlled by the user) recorded during the tests set a (displacement rate of 0.04 mm/s only) are presented in Figure 6 in terms of out-of-plane moment $M_y = H_y \cdot h$. The values are and always relatively small except for paths 1, where high values of M_y are mobilised after the development of large displacement conditions.
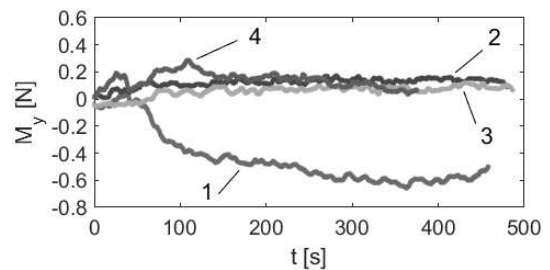

Figure 6.Time history of the out-of-plane moment M_y for each test path (set a).

5. TOWARD A MACROLEMENT MODELLING

In the framework of classical plasticity models, macroelement theories have been widely employed in recent decades to accurately describe complex soil-structure interaction problems at the macro scale of the structural element (Nova and Montrasio, 1991; di Prisco et al., 2003; Gourvernec et al., 2007; Galli et al., 2015; Galli and Mortara, 2021). The authors believe that the experimental results here presented, although still far from allowing the complete definition of a plastic macroelement law for trees, can however provide valid information to extend existing theories to tree root plates (e.g. as in Zhang et al., 2023). Three aspects will be in particular discussed: (i) the limit locus (i.e. the failure condition in a multiaxial loading space), (ii) the hardening law and (iii) the flow rule.

5.1. Limit locus

The envelope of the recorded loading paths into the $M_x - V$ plane provides experimental evidence of a possible shape of the limit locus of the system, i.e. of the failure condition in the load space. Figure 7 shows a view of the four considered paths (only the test set a has been reported). As suggested in the figure, possible comprehensive envelopes are represented by arcs of ellipses (plotted as bold black lines). A

marked asymmetric shape is observed between compression ($V > 0$) and pull-out domains ($V < 0$). Although not experimentally investigated, given to the non-symmetric geometrical shape of the root plate, significant asymmetric shape of the failure locus should also be expected between positive and negative M_x values. Owing to such geometrical asymmetry, vertical paths, both in pull-out and compression cases (paths 2 and 1, respectively), show non-zero mobilised values of the reacting moment M_x until failure is reached. For path 1, in particular, failure is expected to occur at a value of about 100 N, and further increases should then be considered to induce large displacements and second order effects. The failure conditions for compression and pull-out paths can be identified in the figure by points V_1=100N (consistently with Figure 4b, test set *a*) and V_2= –6.5N (with Figure 4c, test set *a*), respectively.
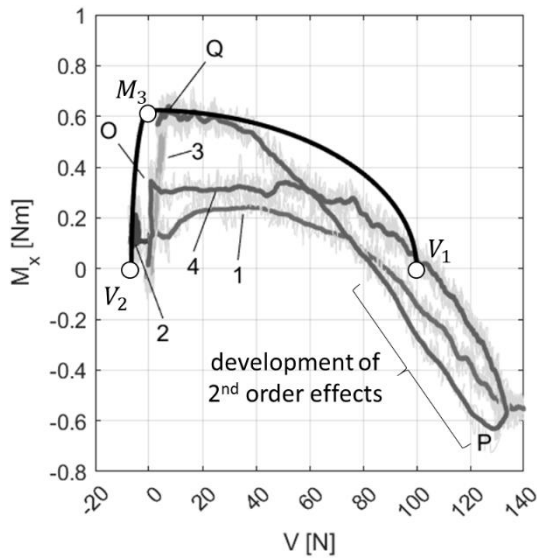

Figure 7. View of the experimental loading paths for the different tests.

When considering path 3 (lateral load) the dominant resisting action is represented by the moment M_x, with only a minor increase in the vertical load V, up to the failure at M_3=0.65Nm. Finally, with reference to path 4, a rather constant value of M_x was initially observed (segment OP, with equal increase in both v and u_x). Once the failure is reached, second order effects take place and the loading path goes well beyond the limit locus. During the second phase (segment PQ), a sudden decrease in V is observed, with a reversal of M_x, reaching the failure around the same point M_3 as path 3.

5.2. Hardening law

The hardening rule in a plastic model controls the evolution of the loading surface, up to the failure condition. In the simplest cases, isotropic hardening is considered, homothetically expanding the loading function. Given this, in Figure 4a a best fit curve based on the equation recently proposed by Galli et al. (2023) has been plotted:

$$\tan\left[\frac{\pi}{2}\left(\frac{M}{M_L}\right)^{1/b}\right] = \frac{\varphi}{\varphi_{70}}\tan\left[\frac{\pi}{2}\left(\frac{\sqrt{2}}{2}\right)^{1/b}\right] \quad (1)$$

Data have been fitted by assuming values of the parameters M_L=0.65Nm (=M_3), φ_{70}=3.3° and b=1, representing the maximum resisting moment value, the rotation of the system at 70% of the maximum resistance and the roundness of the curve, respectively. In the cited paper, the equation was verfied by the Authors to capture important size effects and to control both resistance and deformability properties of the toppling mechanisms. Given its good generality and accuracy, it could be extended to represent a valuable hardening function for strain-hardening plastic models.

5.3. Flow rule

The evolution of settlement and rotation values in a plasticity framework are controlled by the flow rule, expressed as the gradient of a scalar function, playing the role of the so-called plastic potential. As already commented with reference to paths 1 and 2 of Figure 7, non-negligible horizontal reactions are observed, owing to the marked non-axisymmetric shape of the root plate with respect to the stem axis. Similarly, when considering path 3, evident vertical loads are also developed during the test. These phenomena are strictly related to the kinematic behaviour of the system: in vertical paths the tree would tend to develop lateral displacement, while in lateral paths, vertical heave or sink can in general develop, depending on the actual position of the centre of rotation of the tree. The qualitative and quantitative modelling of such complex and coupled mechanisms requires the introduction of a highly refined plastic potential, so that, in general, a non-associative flow rule can be defined. This is beyond the scope of this paper based on the data presented here, but the physical modelling approach here presented may be valuable in developing the required physical data.

6. CONCLUSIONS

This paper presented the results of seven small scale 1g tests on a 3D simplified root prototype. The innovative contribution is related to the possibility of imposing combined displacement-controlled paths, in a multi-axial frame. Vertical (both compression and pull-out) and lateral actions were imposed, to study the moment-rotation and the load-displacement curves. The system exhibits marked non-linear behaviour from the very beginning of the tests, with development of significant second order effects. These latter, while dominating the mechanical response under compression loads, seem not to significantly influence the maximum toppling resistance. No clear evidence of rate-dependent effects was observed, at least for the tested geometry and for the investigated range of displacement rates.

Thedata are fundamental in view of ongoing efforts to develop a 3D formulation of a macroelement law, capturing the main aspects of the mechanical behaviour of root plate systems, under complex and combined loading conditions. With these regards, a preliminary data analysis sugguested a possible shape of the failure locus, and allowed further validation of a newly proposed equation to be employed as hardening function. The requirement of a non associative flow rule was then shortly discussed.
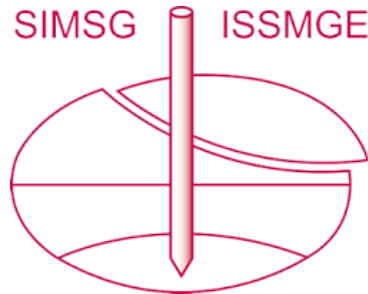
ACKNOWLEDGEMENTS

REFERENCES

Alani, A. M., & Lantini, L. (2020). Recent advances in tree root mapping and assessment using non-destructive testing methods: a focus on ground penetrating radar. *Surveys in Geophysics*, 41, 605-646.

di Prisco C., Nova R., Sibilia A. (2003) – Shallow footing under cyclic loading: experimental behaviour and constitutive modelling. *Geotechnical analysis of the seismic vulnerability of historical monuments, Maugeri M., Nova R. (Eds.)*, Pàtron, Bologna, pp. 99-122.

Dupuy, L., Fourcaud, T., & Stokes, A. (2005). A numerical investigation into the influence of soil type and root architecture on tree anchorage. *Plant and soil*, 278, 119-134. https://doi.org/10.1007/s11104-005-7577-2

Galli A., FarshchI I., Caruso M. (2015) – Influence of loading path on cyclic mechanical response of small-scale shallow strip footing on loose sand. *Canadian Geotechnical Journal*, 52, n. 9, pp. 1228-1240.

Galli, A., Mortara, G.: Experiments and modelling of horizontal loading tests on small scale foundations in sand at constant vertical load. *Géotechnique Letters* 11, 171-178 (2021).

Galli, A., Sala, C., Castellanza, R., Marsiglia, A., & Ciantia, M. O. (2023). Lesson learnt from static pulling tests on trees: an experimental study on toppling behaviour of complex foundations. *Acta Geotechnica*, 1-18. https://doi.org/10.1007/s11440-023-02004-1

Gourvenec S. (2007) – Failure envelopes for offshore shallow foundations under general loading. *Géotechnique*, 57, n.9, pp. 715-72.

Guitard, D. G. E., & Castera, P. (1995). Experimental analysis and mechanical modelling of wind-induced tree sways. *Wind and trees*, 182-194.

Liang, T., Knappett, J. A., & Bengough, A. G. (2014). Scale modelling of plant root systems using 3-D printing. *ICPMG2014–physical modelling in geotechnics*, 1, 361-366.

Liang, T., & Knappett, J. A. (2017). Centrifuge modelling of the influence of slope height on the seismic performance of rooted slopes. *Géotechnique*, 67(10), 855-869. https://doi.org/10.1680/jgeot.16.P.072

Marsiglia, A., Ciantia, M., O., Galli, A., Canepa, D.: Vertical loading tests on a simplified tree root prototype. *Proceedings of the X Int.Conf. on Physical Modelling in Geotechnics*, pp. 832-835, Korean Geotechnical Society, Seoul, Korea (2022).

Marsiglia, A., Galli, A., Marrazzo, G., Castellanza, R., & Ciantia, M. O. (2023). Uprooting Safety Factor of Trees from Static Pulling Tests and Dynamic Monitoring. In *VIII Convegno Nazionale dei Ricercatori di Ingegneria Geotecnica* (pp. 218-225). Springer. https://doi.org/10.1007/978-3-031-34761-0_27

Meijer, G. J., Bengough, A. G., Knappett, J. A., Loades, K. W., & Nicoll, B. C. (2018). In situ measurement of root reinforcement using corkscrew extraction method. *Canadian Geotechnical Journal*, 55(10), 1372-1390.

Nova, R., & Montrasio, L. (1991). Settlements of shallow foundations on sand. *Géotechnique*, 41(2), 243-256.

Riccio, T., Romero, T., Mánica, M., Previtali, M., & Ciantia, M. (2024). A 4D soil-structure interaction model testing apparatus. Submitted to *Geotechnical Testing Journal*, 1(1), 1–12.

Yang, M., Défossez, P., Danjon, F., & Fourcaud, T. (2014). Tree stability under wind: simulating uprooting with root breakage using a finite element method. *Annals of botany*, 114(4), 695-709.

Zhang, X., Knappett, J. A., Leung, A. K., Ciantia, M. O., Liang, T., & Danjon, F. (2020). Small-scale modelling of root-soil interaction of trees under lateral loads. *Plant and Soil*, 456, 289-305.

Zhang, X., Knappett, J. A., Leung, A. K., Ciantia, M. O., Liang, T., & Nicoll, B. C. (2023). Centrifuge modelling of root–soil interaction of laterally loaded trees under different loading conditions. *Géotechnique*, 73(9) 766-780. https://doi.org/10.1680/jgeot.21.00088

INTERNATIONAL SOCIETY FOR SOIL MECHANICS AND GEOTECHNICAL ENGINEERING

The paper was published in the proceedings of the 5th European Conference on Physical Modelling in Geotechnics and was edited by Miguel Angel Cabrera. The conference was held from October 2nd to October 4th 2024 at Delft, the Netherlands.

To see the prologue of the proceedings visit the link below:

https://issmge.org/files/ECPMG2024-Prologue.pdf